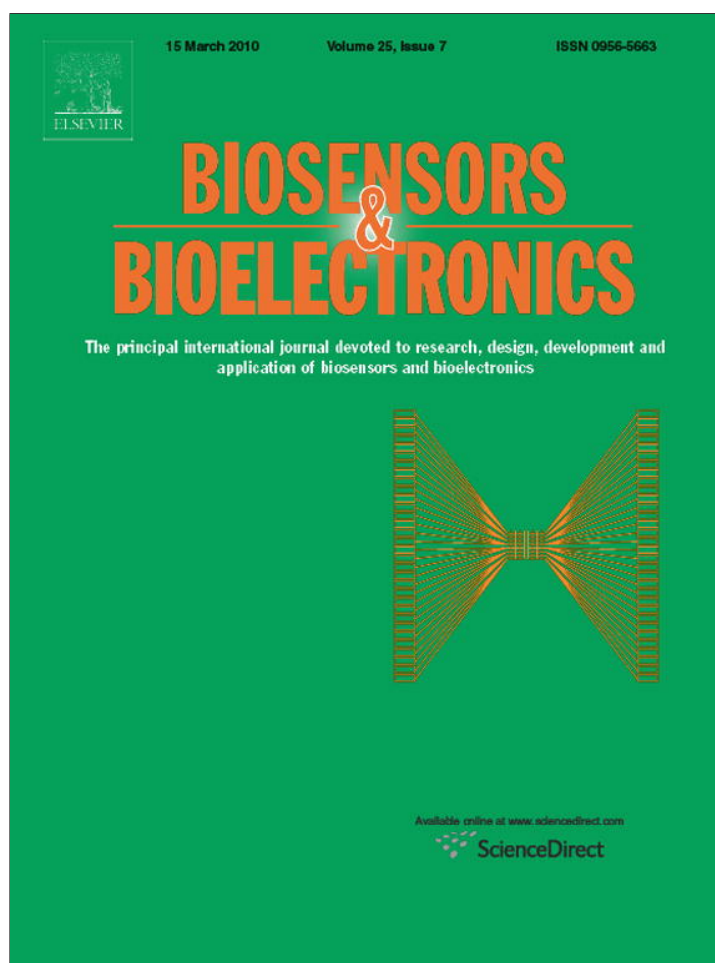


Provided for non-commercial research and education use.  
Not for reproduction, distribution or commercial use.



This article appeared in a journal published by Elsevier. The attached copy is furnished to the author for internal non-commercial research and education use, including for instruction at the authors institution and sharing with colleagues.

Other uses, including reproduction and distribution, or selling or licensing copies, or posting to personal, institutional or third party websites are prohibited.

In most cases authors are permitted to post their version of the article (e.g. in Word or Tex form) to their personal website or institutional repository. Authors requiring further information regarding Elsevier's archiving and manuscript policies are encouraged to visit:

<http://www.elsevier.com/copyright>



Contents lists available at ScienceDirect

## Biosensors and Bioelectronics

journal homepage: [www.elsevier.com/locate/bios](http://www.elsevier.com/locate/bios)

## Nonenzymatic amperometric sensing of glucose by using palladium nanoparticles supported on functional carbon nanotubes

Xiao-mei Chen<sup>a</sup>, Zhi-jie Lin<sup>a</sup>, De-Jun Chen<sup>a</sup>, Tian-tian Jia<sup>a</sup>, Zhi-min Cai<sup>a</sup>, Xiao-ru Wang<sup>a</sup>, Xi Chen<sup>a,b,\*</sup>, Guo-nan Chen<sup>c</sup>, Munetaka Oyama<sup>d</sup>

<sup>a</sup> Department of Chemistry and Key Laboratory of Analytical Sciences of the Ministry of Education, College of Chemistry and Chemical Engineering, Xiamen University, Xiamen 361005, China

<sup>b</sup> State Key Laboratory of Marine Environmental Science, Xiamen University, Xiamen 361005, China

<sup>c</sup> Ministry of Education Key Laboratory of Analysis and Detection Technology for Food Safety, Fuzhou University, Fuzhou 350002, China

<sup>d</sup> Division of Research Initiatives, International Innovation Center, Kyoto University, Nishikyō-ku, Kyoto, 615-8520, Japan

## ARTICLE INFO

## Article history:

Received 26 October 2009

Received in revised form

10 December 2009

Accepted 29 December 2009

Available online 6 January 2010

## Keywords:

Nonenzymatic

Amperometric sensor

Palladium nanoparticles

Glucose

## ABSTRACT

A nonenzymatic electrochemical method was developed for glucose detection using an electrode modified with palladium nanoparticles (PdNPs)-functional carbon nanotubes (FCNTs). PdNPs were homogeneously modified on FCNTs through a facile spontaneous redox reaction and characterized by transmission electron microscopy. Based on the voltammetric and amperometric results, PdNPs efficiently catalyzed the oxidation of glucose at 0.40V in the presence of 0.2M NaCl and showed excellent resistance towards poisoning from such interfering species as ascorbic acid, uric acid, and *p*-acetamidophenol. This anti-poisoning ability was investigated using analysis of the electrocatalytic products by in situ subtractively normalized interfacial Fourier transform infrared reflection spectroscopy, and the results indicated that no strongly adsorbed CO<sub>ad</sub> species could be found in the oxidation products, which was obviously different from the results obtained using Pt-based electrodes. In order to verify the sensor reliability, it was applied to the determination of glucose in urine samples. The results indicated that the proposed approach provided a highly sensitive, wide linear range, more facile method with good reproducibility for glucose determination, promising the development of Pd-based material in nonenzymatic glucose sensing.

© 2010 Elsevier B.V. All rights reserved.

### 1. Introduction

Diabetes mellitus is a chronic but treatable disease affecting about 200 million people around the world (Sljukic et al., 2006). For these patients, regular measurements of blood glucose levels are required to confirm whether the treatments are working effectively (Wang, 2008). As a result, there is an ever-growing demand to create high sensitivity, high reliability, rapid, recyclable and low cost glucose sensors (Sljukic et al., 2006). Electrochemical glucose sensors, especially nonenzymatic amperometric biosensors, hold a leading position among various biosensors.

Direct electrocatalytic oxidation of glucose at a nonenzymatic electrode would exhibit conveniences and advantages to avoid the

enzyme electrode drawbacks. Recently, the interest in a practical nonenzymatic glucose sensor has been centered on the efforts to find a breakthrough in the electrocatalysis. In this context, different substrates, such as platinum (Vassilyev et al., 1985), gold (Li et al., 2007), copper (Luo et al., 1991), alloys (containing Pt, Pb, Au, Pd, Ir and Ru) (Sakamoto and Takamura, 1982; Sun et al., 2001; Aoun et al., 2003; Aoun et al., 2004), and metal oxides (IrO<sub>2</sub>, MnO<sub>2</sub> and CuO) (Irhayem et al., 2002; Chen et al., 2008; Zhuang et al., 2008), have been studied. On the basis of this research, two important clues came to our attention, first, a highly active surface area of the electrode material plays a key role in the electrooxidation of glucose; and second that the poor measurement stability caused by the surface poisoning from adsorbed intermediate products or the effect from co-existing electroactive species such as ascorbic acid (AA), uric acid (UA), and *p*-acetamidophenol (AP), is still a serious problem in the application of nonenzymatic electrodes (Song et al., 2005; Yuan et al., 2005; Jena and Raj, 2006). Therefore, efforts need to be made to find materials with high electrocatalytic activity and good stability in glucose sensing (Park et al., 2003; Bai et al., 2008; Holt-Hindle et al., 2008; Wang et al., 2008a).

\* Corresponding author at: Department of Chemistry and Key Laboratory of Analytical Sciences of the Ministry of Education, College of Chemistry and Chemical Engineering, Xiamen University, Xiamen 361005, China. Tel.: +86 592 2184530; fax: +86 592 2184530.

E-mail address: [xichen@xmu.edu.cn](mailto:xichen@xmu.edu.cn) (X. Chen).

Palladium nanoparticles (PdNPs) are one of the most efficient catalysts in the formation of the C–C bond and chemical transformations such as hydrogenation, hydrodechlorination, carbonylation and oxidation (Lim et al., 2005). Furthermore, the abundance of Pd on the earth is at least 50 times more than that of Pt, which has raised the interest for intensive research on PdNPs in areas of catalysis (Xu et al., 2007). The immobilization of metal nanoparticles to nanotubes is of interest to obtain nanoparticles/nanotube hybrid materials with useful properties (Yang et al., 2007; Wang et al., 2008b). In our previous study, we discovered a facile spontaneous redox method to prepare PdNPs-FCNTs (Chen et al., 2009a), and found that the novel material could catalyze glucose oxidation which enhanced luminol's ECL in neutral solution (Chen et al., 2009b). In the further research, based on voltammetric and amperometric results, we are amazed that the electrocatalytic activity of PdNPs-FCNTs toward glucose oxidation is more excellent in alkaline solution. The results showed that PdNPs-FCNTs revealed high electrocatalytic activity and excellent stability for glucose determination. To further investigate the reason for the high stability achieved on the PdNPs-FCNTs-Nafion modified electrode, we applied a technique called in situ subtractively normalized interfacial fourier transform infrared (SNIFTIR) reflection spectroscopy working with a thin-layer IR cell to monitor the electrooxidation process of glucose on the modified electrode, and found that the oxidation product, CO<sub>2</sub> without adsorbed CO (CO<sub>ad</sub>) species, was quite different from that obtained on a Pt electrode (Beden et al., 1996). To the best of our knowledge, this is the first time that a PdNPs-FCNTs-Nafion electrode has been employed in the development of nonenzymatic amperometric biosensors. This result demonstrated that the applications of a PdNPs-FCNTs-Nafion modified electrode was feasible in glucose detection and indicated a breakthrough in nonenzymatic sensors using Pd-based electrodes.

## 2. Experimental section

### 2.1. Materials

K<sub>2</sub>PdCl<sub>4</sub> was purchased from Wake Pure Chemicals, Co. Ltd. (Osaka, Japan); multiple wall CNTs (MWCNTs) were obtained from Shenzhen Nanotech Port Co. Ltd. (Shenzhen, China); 5% Nafion ethanol solution was from Aldrich Chem. Co. (USA); glucose, AA, UA and AP were from Sinopharm Chemical Reagent Ltd. Co. (Guangzhou, China); and rod glassy carbon electrodes (GCEs) were from BAS Co. Ltd. (Tokyo, Japan). All other reagents were of analytical grade and used without further purification. The pure water for solution preparation was from a Millipore Autopure WR600A system (Millipore, Ltd., USA).

### 2.2. Instrumentations

Morphologies of PdNPs-FCNTs were examined using a high resolution transmission electron microscope (HRTEM, FEI Tecnai-F30 FEG). Energy dispersive X-ray spectroscopy (EDX) analysis was used to identify the elemental composition of the complex. Electrochemical SNIFTIR reflection spectroscopic studies were carried out on a Nexus 870 spectrometer (Nicolet) equipped with a liquid-nitrogen-cooled MCT-A detector and an EverGlo IR source. The configuration of the thin-layer IR cell was described previously by Zhou et al. (2008) (see the details in Supporting Information). Electrochemical measurements were performed with a CHI 660B Electrochemical Analyzer (CHI Co. Shanghai, China). The conventional three-electrode system included a GCE coated with PdNPs-FCNTs-Nafion film, a platinum auxiliary electrode and a saturated calomel reference electrode.

### 2.3. Procedure

Decoration of PdNPs onto FCNTs was achieved using the spontaneous redox method based on our previous studies (Tao et al., 2008; Chen et al., 2009a). A vial containing FCNTs (0.5 mL 0.5 mg mL<sup>-1</sup>) and K<sub>2</sub>PdCl<sub>4</sub> (0.5 mL 10 mM) aqueous solution was kept in an oil bath at 70 °C under vigorous stirring for 30 min. Then, the reaction mixture was washed with pure water and centrifuged to remove the remaining reagents. Finally, the PdNPs-FCNTs were dispersed in pure water (0.5 mL). Before the preparation of the PdNPs-FCNTs-Nafion modified GCE, the GCE was polished with 1, 0.3 and 0.05 μm α-Al<sub>2</sub>O<sub>3</sub>, sequentially. After ultrasonic concussion, the polished GC electrode was dried at room temperature. During the coating of the PdNPs-FCNTs nanocomposite onto the GCE surface, PdNPs-FCNTs suspension (30 μL) was dispersed into Nafion (30 μL 0.5%) ethanol solution, 2 μL PdNPs-FCNTs-Nafion suspension was then dropped onto the GCE surface, and it was subsequently dried in the air for 4 h at room temperature. During electrochemical measurements, the working area of the modified GCE was 7.0 mm<sup>2</sup>, and the density of PdNPs-FCNTs deposited on the electrode was 7.1 μg cm<sup>-2</sup>.

## 3. Results and discussion

### 3.1. Characterization of the PdNPs-FCNTs

Direct morphological observation of the as-prepared PdNPs attachment to the surface of the FCNTs was made using a TEM. A typical TEM picture is shown in Fig. 1. In the figure, we can see that many Pd dots grow on the broken or peristome positions of the FCNTs, in which there is a higher density of hydroxyl groups (Xing et al., 2005). It is surprising that PdNPs congregated together to form several spheres on the surfaces of the FCNTs, giving them the appearance of a tree in bloom. From the HRTEM image (Fig. 1b), it is quite clear that PdNPs formed in the spheres were well separated and the average size of the dots was around 3–4 nm. This image revealed that PdNPs were well attached onto the FCNT surfaces. In addition, an obvious Pd peak found from the EDX experiment, as shown in Fig. 1a (inset), further confirmed this result.

### 3.2. Electrocatalytic oxidation of glucose

The cyclic voltammogram (CV) method was used to compare and investigate the catalytic activity of the as-prepared PdNPs-FCNTs-Nafion modified electrodes. Fig. 2a presents the CV responses on a PdNPs-FCNTs-Nafion modified electrode in 0.1 M NaOH-0.2 M NaCl solution with and without 100 mM glucose. The current–potential profile of the modified electrode in the NaOH–NaCl solution was almost featureless. The current at a potential of –0.1 V was due to the formation of Pd–OH and the rapidly increased current around a potential above 0.6 V corresponding with the metal oxide formation. The single cathodic peak (which started from –0.34 V) was related to the reduction of dissolved oxygen in solution and the Pd oxide formed in the positive scan at 0.6 V. This deduction could be confirmed by the result that the cathodic peak decreased obviously (Figure S1) when the solution was bubbled with N<sub>2</sub> for 20 min. In comparison, the CV curve for glucose in the solution was complicated. In the positive direction scan of the applied potential, two anodic peaks located at –0.12 V and 0.45 V were shown in the curve. The former could be attributed to the glucose electroadsorption causing the generation of an adsorbed intermediate, and per glucose molecule lost one proton in this electrochemical reaction. As the reaction continued, the accumulation of the intermediates on the electrode surface inhibited further the electroadsorption of glucose, resulting in a decrease in current. When the applied potential was larger than 0.30 V, Pd(OH)<sub>x</sub> species

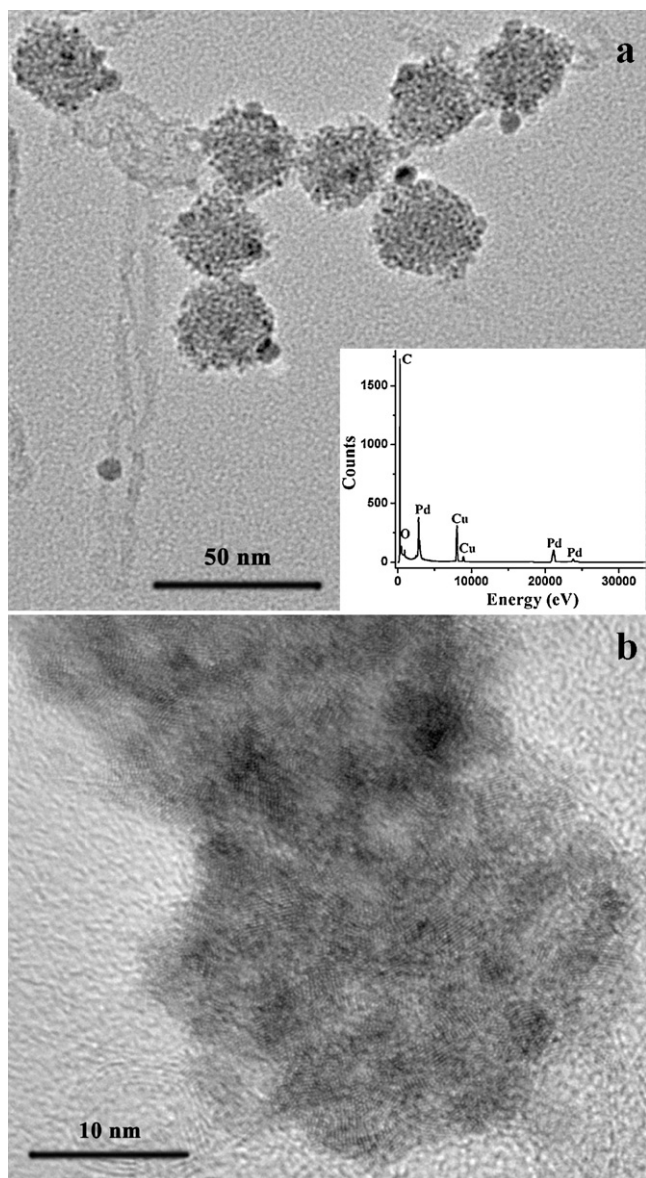


**Fig. 1.** TEM (a) and HRTEM (b) image of PdNPs-FCNTs. The inset shows the EDX spectra of PdNPs-FCNTs.

were generated in the alkaline solution. Pd(OH)<sub>x</sub> is beneficial in oxidizing the poisoning intermediates derived from the glucose electroadsorption. This process released free active PdNP sites for the direct oxidation of glucose, which was similar to the case with the electrochemical oxidation of ethanol (Xia et al., 1996; Xia et al., 1997). Therefore, the electrooxidation current for glucose increased again due to the direct oxidation of glucose on the oxidized PdNP surfaces, and simultaneously, the second current peak appeared at 0.45 V. The current decreased at a higher applied potential owing to the evolution of oxygen on the Pd surface, and oxygen covered the active sites on the PdNPs. In the negative scan, two peaks appeared in the curves. In the range +0.70 to −0.34 V, the oxidation of glucose was suppressed due to the oxidation of PdNP surfaces. The oxidized Pd surfaces were reduced at a potential around −0.34 V, and their activity began to show more recovery. With the continuing negative scan, more surface-active sites were renewed and became available for the oxidation of glucose, resulting in a large anodic peak in the potential range from −0.40 to −0.55 V. Synchronously, at a potential of −0.45 V, the accumulation of intermediates and the adsorption of H atoms again occurred, inducing current decrease.

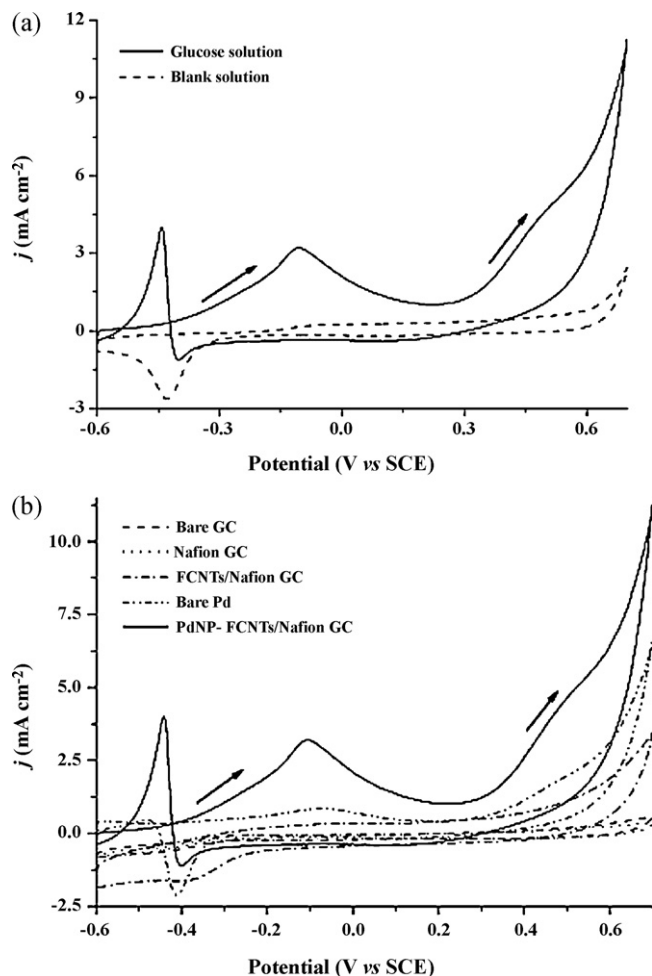


**Fig. 2.** (a) CV curves of the PdNPs-FCNTs-Nafion electrode in the solution with and without glucose. (b) CV curves in NaOH-NaCl glucose solution on different electrodes. Scan rate: 60 mV s<sup>−1</sup>; glucose: 100 mM; NaCl: 0.2 M; NaOH: 0.1 M.

It should be pointed out that the catalytic peak here was only obtained at higher concentrations of glucose (>1 mM) and could not be observed in the micromolar range. The above results could be further confirmed by comparing the responses of the solution under an N<sub>2</sub> atmosphere and applying various initial potentials during negative scans (Figure S1 and Figure S2). With N<sub>2</sub> insufflated, the catalytic peak at around −0.45 V obviously increased since oxygen concentration decreased in the solution. This result revealed that the catalytic peak appearing in CV curves was the additive result of the electrocatalytic oxidation of glucose. Different initial potential toward negative scans, from 0.0 to 0.8 V, caused a different LSV curve. Higher initial potential applied during negative scans seemed helpful in the oxidation of the intermediate products accumulating on the electrode. In the experiment, the electrocatalytic peak increased when an initial potential from 0.0 to 0.6 V was selected. In the LSV scan, a greater amount of Pd oxide was produced when a positive initial potential (>0.6 V) was applied, and more distinct reduction behavior could be found from −0.3 V. This means that the catalytic peak appearing in the CV curve should counteract more reduction current, and finally, the catalytic peak decreased when the applied initial potential was more positive than 0.6 V.

We further investigated the effect of different electrode materials on glucose oxidation. Fig. 2b compares the voltammograms obtained from the oxidation of glucose by a bare GC, a Nafion-GC, a FCNTs/Nafion-GC, a bare Pd and a PdNPs-FCNTs-Nafion modified electrode. As can be seen from the CV curves, no obvious oxidation

currents for glucose could be found on the first three electrodes. However, both the bare Pd and the PdNPs-FCNTs-Nafion modified electrode exhibited typical voltammetric responses for glucose, suggesting that Pd played a key role in the CV feature. In Fig. 2b, two obvious oxidation peaks in the anodic scan and one peak in the cathodic scan indicated the catalytic ability of the two kinds of electrodes toward glucose oxidation. The current density of the oxidation peak achieved at 0.45,  $-0.1$  and  $-0.45$  V on the PdNPs-FCNTs-Nafion modified electrode was about 3.5, 10 and 15 folds than those obtained on the bare Pd electrode. Generally, a higher electrooxidation current intensity of glucose could be obtained by a larger real surface area of the electrode (Frelink et al., 1995), since the electrochemical reaction is kinetically controlled. It could be considered that PdNPs in the glucose oxidation process had a surface-like behavior, and that their large ratio of area-to-volume could effectively enhance the reaction. Moreover, as a bifunctional mechanism in biometallic nanoparticles, hydroxyl groups on FCNTs could benefit the oxidation of the poisoning intermediates derives from the glucose electroadsorption, resulting in the improvement of the sensor stability. The results illustrate that a PdNPs-FCNTs-Nafion modified electrode presented the best catalytic performance among the five electrodes tested.

### 3.3. Amperometric sensing of glucose

In the evaluation of an amperometric sensor, current responses were measured under different concentrations of the objective analyte at a fixed potential and at fixed times. To improve the performance of the glucose sensor, several factors such as NaOH concentration (Figure S3) and the applied potential (Fig. 3) were optimized. In the alkaline solution, Pd played its catalytic role efficiently. This deduction could be further confirmed from the CV result of the glucose solution containing 0.5 M  $\text{H}_2\text{SO}_4$  where no obvious catalytic peak could be found in the CV curve, which indicates that  $\text{OH}^-$  plays an important role in glucose oxidation on the PdNPs-FCNTs-Nafion modified electrode. Although a higher concentration of  $\text{OH}^-$  in the solution caused higher electrocatalytic activity of Pd, on the contrary, too much  $\text{OH}^-$  blocked the further electroadsorption of glucose anion (per glucose molecule lost one proton at about  $-0.12$  V, the accumulation of glucose anions could enhance the current responses), resulting in a decrease in current. As a result, 0.1 M NaOH was selected for the electrocatalytic oxidation of glucose.

Based on the above results, successive addition of 20.0  $\mu\text{L}$  1.0 M glucose (final volume 10.0 mL) to the solution was performed at applied potentials of 0.40 and  $-0.06$  V, and the corresponding electrochemical response was recorded while the solution was stirred constantly. As shown in Fig. 3a, at  $-0.06$  V, the current density increased during the first 13 injections of glucose (2 mM increase for each injection) and then became unstable when more glucose was injected; whereas, at 0.40 V, the current density increased with the increase of glucose from 0 to 46 mM (Fig. 3b). In addition, the current density at 0.40 V was much higher than that at  $-0.06$  V for each glucose addition. The current density ratio came up to around 50. From this feature, shown in Fig. 3a, it can be reasonably interpreted that glucose cannot be completely oxidized at the potential of  $-0.06$  V, resulting in the formation of intermediates on the electrode surface. The intermediates poison the active catalytic sites of the PdNPs, and cause the amperometric response to become unstable and to decrease. In contrast, as shown in Fig. 3b, the higher response to glucose oxidation at 0.40 V indicated a better sensitivity in glucose sensing. In the inset of Fig. 3b, the linear dependence of current density with glucose concentration at 0.40 V gives  $11.4 \mu\text{A cm}^{-2} \text{ mL mol}^{-1}$ , revealing that it is more sensitive than that at  $-0.06$  V ( $0.24 \mu\text{A cm}^{-2} \text{ mL mol}^{-1}$ ). Moreover, the current density at 0.40 V presented a better lin-

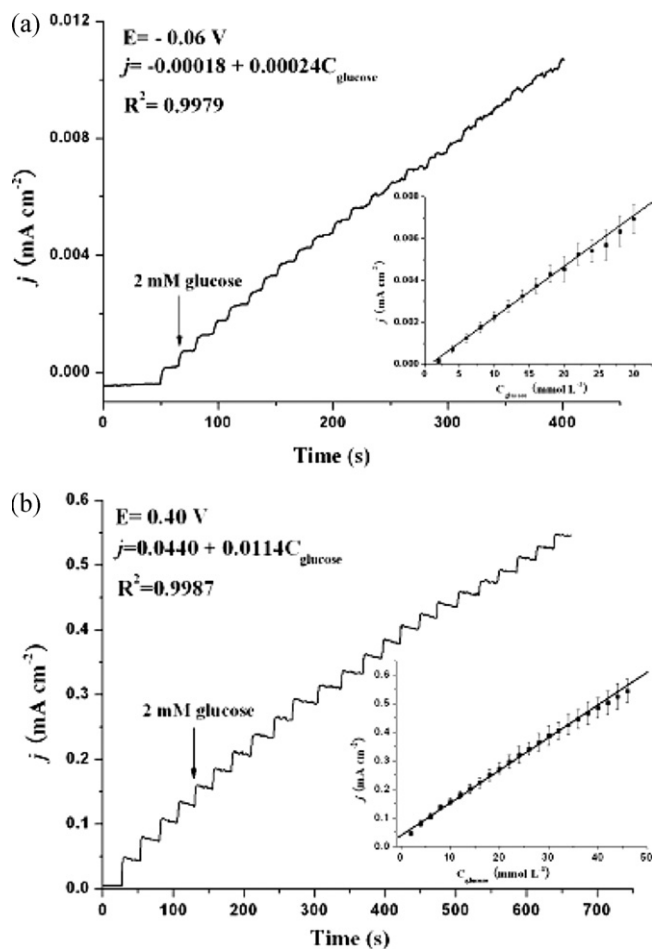
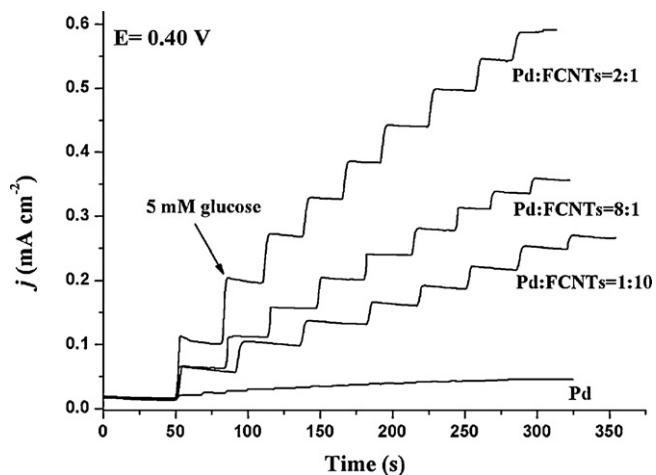


Fig. 3. Chronoamperometry curves of the PdNPs-FCNTs-Nafion electrode with the successive addition of 2 mM glucose. The applied potential was  $-0.06$  V (a) and 0.40 V (b). The inset shows the calibration curve of glucose concentration and plateau currents at  $-0.06$  V (a) and 0.40 V (b). NaCl: 0.2 M; NaOH: 0.1 M.

earity with glucose concentration ranging from 0 to 46 mM with a correlation coefficient of 0.9987. To the best of our knowledge, the amperometric responses of the PdNPs-FCNTs-Nafion modified electrode at 0.40 V has the highest sensitivity and the widest detection range so far seen in the literature on Pd-based electrodes. The advantages could also be supported by comparison with other nonenzymatic glucose sensor as showed in Table S2.

We further investigated the amperometric responses in glucose sensing with different weight ratios between Pd and FCNTs on PdNPs-FCNTs-Nafion modified electrodes at the optimum potential of 0.40 V. As shown in Fig. 4, the bare Pd electrode showed the worst sensitivity among all the electrodes tested with the successive addition of 5 mM glucose because of the poisoning by electroadsorption intermediates and chloride ions. The PdNPs-FCNTs-Nafion modified electrodes revealed much higher current responses than those from the bare Pd electrode since (1) the high active surface area on PdNPs noticeably enhanced glucose electrooxidation; (2) FCNTs might enhance the mass transport of glucose to active PdNP surfaces, which would also benefit glucose electrooxidation. The results in Fig. 4 display that all the PdNPs-FCNTs-Nafion modified electrodes presented linear amperometric responses and the sensitivity increased in the following order: Pd-FCNTs (2:1) > Pd-FCNTs (8:1) > Pd-FCNTs (1:10), indicating that the Pd-FCNTs (2:1) gave the optimal composition for glucose sensing and detection.



**Fig. 4.** Chronoamperometry curves of glucose at PdNPs-FCNTs-Nafion electrodes with different weight ratios between Pd and FCNTs. NaCl: 0.2 M; NaOH: 0.1 M; potential: 0.4 V; the successive addition of glucose: 5 mM.

### 3.4. Evaluation of the modified electrode

As mentioned in the introduction, one of the major challenges in nonenzymatic glucose detection is the interfering electrochemical signals caused by some easily oxidizable compounds such as AA, UA, and AP. It has been reported that the overall kinetics of glucose electrooxidation is too sluggish to produce significant faradaic currents on a smooth Pt electrode (Lei et al., 1995). In addition, despite the fact that glucose concentration (3–8 mM) is much higher than those of AA (0.1 mM), UA (0.02 mM) and AP (0.1 mM) in a normal physiological sample, these interfering species can generate oxidation currents comparable to that of glucose, because their electron transfer rates are considerably faster than that of glucose (Park et al., 2003). On the other hand, high active surface area favors faradaic currents associated with kinetically controlled sluggish reactions (the oxidation of glucose) to a greater extent than a diffusion controlled reactions (the oxidation of interfering species) (Park et al., 2003; Yuan et al., 2005). This characteristic indicates that nanostructure electrodes can be applied to conquer the poor selective problem met with in nonenzymatic glucose sensing. To test this, we further studied the CV behaviors of the PdNPs-FCNTs-Nafion modified electrode in the presence of 0.1 mM AA, and 1.0 mM glucose in 0.1 M NaOH containing 0.2 M NaCl. From the CV curves shown in Fig. 5, the current density peak at 0.45 V of glucose is about 5 fold higher than that of AA, which shows its ability to avoid the interfering current signal contributed by AA. For further comparison, we investigated the amperometric response on PdNPs-FCNTs-Nafion modified electrodes with successive additions of UA, AP, AA, and glucose. As presented in the inset, glucose produced remarkable signals comparing to the other three interfering species. If the current density of glucose was set as 100%, the interference current density from UA, AP or AA was only 1.8%, 2.0% or 6.5%, respectively. This result demonstrated that electrochemical detection of glucose on PdNPs-FCNTs-Nafion modified electrodes could be performed with negligible interference from UA, AP, and AA under the present conditions.

Most electrochemical glucose sensors are based on metals or alloys which easily lose their activity due to poisoning by chloride ions (Aoun et al., 2003; Li et al., 2007). In order to understand whether chloride ions poison the electrocatalytic ability of the PdNPs-FCNTs-Nafion modified electrode for glucose oxidation, we studied the amperometric responses in solutions containing various concentrations of NaCl (0, 0.05, 0.1, 0.15, 0.2 and 0.3 M) (Figure S4). It has been reported that in the presence of  $\text{Cl}^-$ , part of

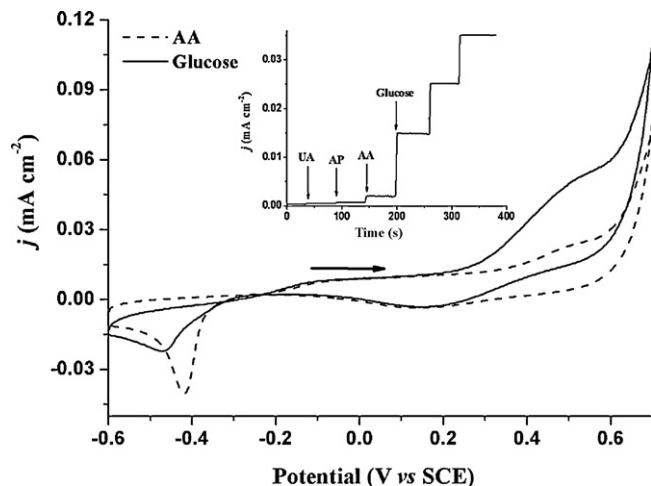


**Fig. 5.** CV curves of the PdNPs-FCNTs-Nafion electrode in glucose (solid line) and AA (dashed line) solutions. The inset shows chronoamperometry curves of the PdNPs-FCNTs-Nafion electrode with the successive addition of 0.02 mM UA, 0.1 mM AP, 0.1 mM AA and 1.0 mM glucose. NaCl: 0.2 M; NaOH: 0.1 M.

the surface-active sites could be preferentially blocked, causing less chance of reactive species approaching the electrode surface (Aoun et al., 2004). However, in our experiment, the PdNPs-FCNTs-Nafion modified electrode could still make a rather strong and stable current signal even in a concentration of  $0.3 \text{ M Cl}^-$ , which is larger than the physiological value (0.16 M). Although this phenomenon was also reported by other researchers, its mechanism is still unclear (Song et al., 2005; Wang et al., 2008a; Bai et al., 2008). In the modified electrode, Nafion containing sulfonic groups may be useful in preventing the poisoning of PdNPs by  $\text{Cl}^-$  and  $\text{OH}^-$  in alkaline solution so can be helpful in resisting poisoning by  $\text{Cl}^-$ .

The long-term storage and operational stability of the electrode is essential for the continuous monitoring of glucose. The stability of the present electrode was examined using the same PdNPs-FCNTs-Nafion modified electrode for 10 repetitive measurements in successive additions of 2 mM glucose at 0.40 V. The relative standard deviation was 4.31%, confirming that the as synthesized electrode for glucose sensing was stable. The long-term storage was evaluated by measuring its sensitivity to glucose over a 10 day period. The sensor was stored in air and the sensitivity was tested every 2 days. The result demonstrated that the sensitivity was 90% of its initial sensitivity after 10 days. These results indicated that the PdNPs-FCNTs-Nafion electrode displays good long-term storage ability and excellent stability, promising a desirable glucose sensor for most routine analyses.

In order to verify the sensor reliability, the recovery of glucose in urine samples was testified. Varying amounts of glucose was added to the urine samples, the potential was hold at 0.40 V with pH 13. As shown in Table S3, the results showed that the PdNPs-FCNTs-Nafion glucose biosensor could be used for the determination of glucose, with satisfactory recoveries of 95.1–105.0%.

### 3.5. Proposed mechanism of glucose electrooxidation

For further study of the high resistant ability of the PdNPs-FCNTs-Nafion modified electrode against poisons, we employed SNIFTIR reflection spectroscopy working with a thin-layer IR cell to monitor the electrooxidation process of glucose on the electrode. Fig. 6 illustrates the SNIFTIR spectra of glucose oxidation on a PdNPs-FCNTs-Nafion electrode at potentials varying from  $-0.30 \text{ V}$  to  $0.50 \text{ V}$ . The assignments of IR bands are listed in Table S1. Five IR bands at 1063, 1092, 1136, 1347 and  $1411 \text{ cm}^{-1}$  can be assigned to the characteristic IR absorption of glucose, which is consistent with

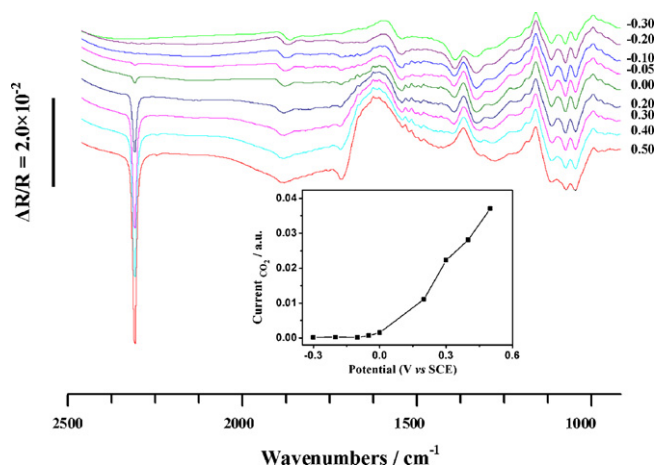


**Fig. 6.** SNIFTIR spectra of glucose electrooxidation on the PdNPs-FCNTs electrode at different potentials.  $E_S$  was varied from  $-0.30$  V to  $0.50$  V. Glucose:  $100$  mM; NaCl:  $0.2$  M; NaOH:  $0.1$  M;  $E_R$ :  $-0.65$  V;  $1000$  scans;  $8$   $\text{cm}^{-1}$ . The inset shows potential dependence of the change in relative concentration of  $\text{CO}_2$ .

glucose oxidation on a Pt electrode (Beden et al., 1996). The downward band at  $2344$   $\text{cm}^{-1}$  is ascribed to IR absorption of  $\text{CO}_2$ , which is the oxidation product of glucose. Interestingly, there is no peak at about  $2041$   $\text{cm}^{-1}$ , indicating that linearly bonded CO ( $\text{CO}_L$ ) could not be produced in glucose oxidation on the PdNPs-FCNTs-Nafion modified electrode. It is different from the SNIFTIR spectra achieved on a Pt electrode (Beden et al., 1996). Unlike  $\text{CO}_2$ ,  $\text{CO}_L$  is a strong-adsorption species on noble metal, which blocks the active sites seriously during catalysis processes (Fukuoka et al., 2007). According to this result, the glucose sensor as synthesized was revealed to be more stable than Pt-based sensors. The dissolved product of  $\text{CO}_2$  at different potentials can be analyzed quantitatively from SNIFTIR spectra (Fig. 6 inset). In brief, the contribution of  $\text{CO}_2$  to the SNIFTIR spectra was evaluated by subtracting its individual transmission spectrum collected in the same liquid-film thickness on an electrode. Thus, the change in relative concentration of  $\text{CO}_2$  in the thin-layer solution was obtained. At  $0.00$  V,  $\text{CO}_2$  could be detected, which was more negative than that on the Pt electrode (Beden et al., 1996), illustrating the high electroactivity of glucose oxidation achieved on the PdNPs-FCNTs-Nafion modified electrode. Along with increasing electrode potential, the intensity of  $\text{CO}_2$  increased quickly and reached a maximum at around  $0.50$  V, demonstrating that glucose exhibited its highest reactivity at  $0.50$  V. In addition, when the potential was higher than  $-0.10$  V (Fig. 6 inset), the production of  $\text{CO}_2$  was obviously different from the current increase of glucose electrooxidation. This result indicated that glucose oxidation should contain a process of decarbonization. Further study of the mechanism of glucose oxidation on PdNPs-FCNTs-Nafion modified electrodes at the molecular level is in progress.

#### 4. Conclusion

In summary, we developed a nonenzymatic glucose sensor based on a PdNPs-FCNTs-Nafion modified electrode. TEM images showed that PdNPs were separated well on the spheres growing on the FCNTs. Direct glucose oxidation on the modified electrode was investigated using voltammetric and amperometric methods. As a result, we found that the modified electrode exhibited high electrocatalytic ability to glucose oxidation in alkaline solution. There are many advantages in employ the modified electrode for glucose sensing detection including (1) it is easy to synthesize PdNPs-FCNTs; (2) the sensing approach had high sensitivity even in

the presence of  $\text{Cl}^-$  and excellent ability to resist some interfering species such as AA, UA, and AP; and (3) without adsorbed CO ( $\text{CO}_{ad}$ ) species in the oxidation product, it avoids the strong adsorption of  $\text{CO}_{ad}$  on the active sites of PdNPs, resulting in long-term stability for glucose sensing. In view of the physiological level of glucose, the wide linear concentration range of glucose ( $0$ – $46$  mM) with a sensitivity of  $11.4$   $\mu\text{A cm}^{-2} \text{mL mol}^{-1}$  was obviously good enough for clinical application.

#### Acknowledgements

This work was financially supported by the National Natural Science Foundation of China (Nos. 20775064, 20735002 and 20975085), the NFFTBS (No. J0630429) and the National Basic Research Program of China (2010CB732402), all of which are gratefully acknowledged. Furthermore, we would like to extend our thanks to Professor John Hodgkiss of The University of Hong Kong for his assistance with English.

#### Appendix A. Supplementary data

Supplementary data associated with this article can be found, in the online version, at doi:10.1016/j.bios.2009.12.035.

#### References

- Aoun, S.B., Bang, G.S., Koga, T., Nonaka, Y., Sotomura, T., Taniguchi, I., 2003. *Electrochem. Commun.* 5, 317–320.
- Aoun, S.B., Dursun, Z., Koga, T., Bang, G.S., Sotomura, T., Taniguchi, I., 2004. *J. Electroanal. Chem.* 567, 175–183.
- Bai, Y., Sun, Y.Y., Sun, C.Q., 2008. *Biosens. Bioelectron.* 24, 579–585.
- Beden, B., Largeaud, F., Kokoh, K.B., Lamy, C., 1996. *Electrochim. Acta* 41, 701–709.
- Chen, J., Zhang, W.D., Ye, J.S., 2008. *Electrochem. Commun.* 10, 1268–1271.
- Chen, X.M., Cai, Z.M., Lin, Z.J., Jia, T.T., Liu, H.Z., Jiang, Y.Q., Chen, X., 2009a. *Biosens. Bioelectron.* 24, 3475–3480.
- Chen, X.M., Lin, Z.J., Jia, T.T., Cai, Z.M., Huang, X.L., Jiang, Y.Q., Chen, X., Chen, G.N., 2009b. *Anal. Chim. Acta* 650, 54–58.
- Frelink, T., Visscher, W., Vanveen, J.A.R., 1995. *J. Electroanal. Chem.* 382, 65–72.
- Fukuoka, A., Kimura, J., Oshio, T., Sakamoto, Y., Ichikawa, M., 2007. *J. Am. Chem. Soc.* 129, 10120–10125.
- Holt-Hindle, P., Nigro, S., Asmussen, M., Chen, A.C., 2008. *Electrochem. Commun.* 10, 1438–1441.
- Irhayem, E.A., Elzanowska, H., Jhas, A.S., Skrzynecka, B., Birss, V., 2002. *J. Electroanal. Chem.* 538–539, 153–164.
- Jena, B.K., Raj, C.R., 2006. *Chem. Eur. J.* 12, 2702–2708.
- Lei, H.W., Wu, B.L., Cha, C.S., Kita, H., 1995. *J. Electroanal. Chem.* 382, 103–110.
- Li, Y., Song, Y.Y., Yang, C., Xia, X.H., 2007. *Electrochem. Commun.* 9, 981–988.
- Lim, S.H., Wei, J., Lin, J.Y., Li, Q.T., You, J.K., 2005. *Biosens. Bioelectron.* 20, 2341–2346.
- Luo, P., Zhang, F., Baldwin, R.P., 1991. *Anal. Chim. Acta* 244, 169–178.
- Park, S., Chung, T.D., Kim, H.C., 2003. *Anal. Chem.* 75, 3046–3049.
- Sakamoto, M., Takamura, K., 1982. *Bioelectrochem. Bioenerg.* 9, 571–582.
- Sljukic, B., Banks, C.E., Salter, C., Crossley, A., Compton, R.G., 2006. *Analyst* 131, 670–677.
- Song, Y.Y., Zhang, D., Gao, W., Xia, X.H., 2005. *Chem. Eur. J.* 11, 2177–2182.
- Sun, Y., Buck, H., Mallouk, T.E., 2001. *Anal. Chem.* 73, 1599–1604.
- Tao, Y., Lin, Z.J., Chen, X.M., Huang, X.L., Oyama, M., Chen, X., Wang, X.R., 2008. *Sens. Actuators B: Chem.* 129, 758–763.
- Vassilyev, Y.B., Khazova, O.A., Nikolaeva, N.N., 1985. *J. Electroanal. Chem.* 196, 105–125.
- Wang, J., 2008. *Chem. Rev.* 108, 814–825.
- Wang, J.J., Yin, G.P., Shao, Y.Y., Wang, Z.B., Gao, Y.Z., 2008a. *J. Phys. Chem. C* 112, 5784–5789.
- Wang, J.P., Thomas, D.F., Chen, A.C., 2008b. *Anal. Chem.* 80, 997–1004.
- Xia, X.H., Iwasita, T., Ge, F.Y., Vielstich, W., 1996. *Electrochim. Acta* 41, 711–718.
- Xia, X.H., Iwasita, T., Liess, H.D., Vielstich, W., 1997. *J. Phys. Chem. B* 101, 7542–7547.
- Xing, Y.C., Li, L., Chusuei, C.C., Hull, R.V., 2005. *Langmuir* 21, 4185–4190.
- Xu, C.W., Cheng, L.Q., Shen, P.K., Liu, Y.L., 2007. *Electrochem. Commun.* 9, 997–1001.
- Yang, L.X., Yang, W.Y., Cai, Q.Y., 2007. *J. Phys. Chem. C* 111, 16613–16617.
- Yuan, J.H., Wang, K., Xia, X.H., 2005. *Adv. Funct. Mater.* 15, 803–809.
- Zhou, Z.Y., Chen, D.J., Li, H., Wang, Q., Sun, S.G., 2008. *J. Phys. Chem. C* 112, 19012–19017.
- Zhuang, Z.J., Su, X.D., Yuan, H.Y., Sun, Q., Xiao, D., Choi, M.M.F., 2008. *Analyst* 133, 126–132.